A Novel Single-Layer Winding Array and Receiver Coil Structure for Contactless Battery Charging Systems With Free-Positioning and Localized Charging Features

W. X. Zhong, Xun Liu, *Member, IEEE*, and S. Y. Ron Hui, *Fellow, IEEE*

***Abstract*—The planar contactless battery charging system is an emerging technology that can be applied to a wide range of portable consumer electronic products. Beginning with a brief historical background, this paper presents a new single-layer winding array and receiver coil structure with cylindrical ferrite cores for planar contactless battery charging systems. Complying with the "Qi" standard, this design enables multiple devices to be placed and charged simultaneously on the wireless charging pad in a free-positioning manner. The charging flux is totally localized within the covered area between the selected primary winding and the secondary winding inside the load. The electromagnetic characteristics of such winding design are studied in finite-element analysis and confirmed by practical implementation.**

***Index Terms*—Contactless battery charging, Qi wireless power standard, wireless power transfer.**

I. Introduction

ELECTRONIC waste caused by the large variety of battery chargers for portable consumer electronic products has become an increasing global problem. One promising way to reduce such electronic waste is the wireless charging technology which has the potential of unifying the charging protocol for a wide range of portable electronic products. The formation of the Wireless Power Consortium (WPC) in November 2008 aims at setting a new common platform for wireless power transfer [1]. In April 2010, the WPC endorsed Part 1 of the world's first international standard on wireless power transfer. The version 1.0 of this standard is set for wireless charging systems with planar charging surfaces. That is, the wireless charging system should have a designated planar area within which a load or several loads can be placed and charged. The new standard is called "Qi" which stands for invisible force in Chinese. Part 1 of the Qi standard is designed primarily for portable electronic devices such as mobile phones and Bluetooth devices with a charging power of up to 5 W. According to the WPC Web site [1], the Qi standard includes three wireless charging approaches:

1) guided positioning charging based on magnetic attraction without a movable mechanical part [see Fig. 1(a)];
2) free-positioning charging for a single device using a movable primary coil underneath the charging surface to locate the device [see Fig. 1(b)];
3) free position for charging single or multiple devices using a winding array without movable mechanical parts [see Fig. 1(c)].

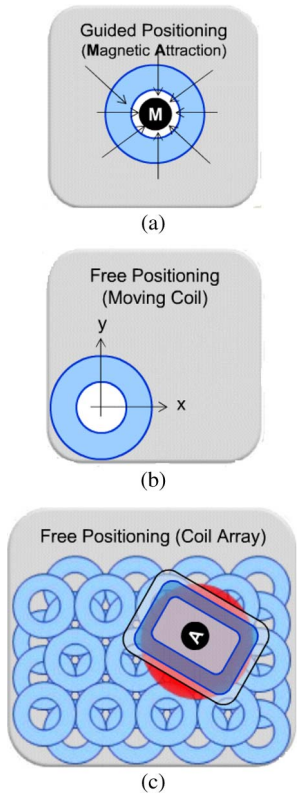

Fig. 1. (a) Approach 1: Guided positioning charging [1]. (b) Approach 2: Free positioning based on a mechanically movable primary coil [1]. (c) Approach 3: Free positioning based on selective excitation of coil array [1], [8], [9], [23], [24].

Manuscript received August 22, 2010; accepted October 28, 2010. Date of publication December 10, 2010; date of current version August 12, 2011. This work was supported by the Hong Kong Research Grant Council under Project CityU 114708.

W. X. Zhong is with the Center for Power Electronics, Department of Electronic Engineering, City University of Hong Kong, Kowloon, Hong Kong (e-mail: eeronhui@cityu.edu.hk).

X. Liu is with the ConvenientPower HK Ltd., Shatin, Hong Kong (e-mail: xun.liu@convenientpower.com).

S. Y. R. Hui is with the Center for Power Electronics, Department of Electronic Engineering, City University of Hong Kong, Kowloon, Hong Kong, and also with the Department of Electrical and Electronic Engineering, Imperial College London, SW7 2AZ London, U.K. (e-mail: r.hui@imperial.ac.uk).

Color versions of one or more of the figures in this paper are available online at http://ieeexplore.ieee.org.

Digital Object Identifier 10.1109/TIE.2010.2098379

Approach 1 is a standard fixed-positioning method that has been used in some existing electric products such as electric toothbrushes. In such applications, the loads are guided into a fixed location by magnetic attraction. In the Qi standard, this approach requires the load to be placed in a fixed location. It features "one-to-one" and "fixed-positioning" charging, i.e., one primary coil transfers to only one secondary coil (housed inside the load) in a fixed position. If the load is not placed directly and precisely on top of the primary coil, the mutual coupling and energy transfer efficiency can deteriorate with the misalignment of the transmitter and receiver coils. Since it is essential to ensure that the primary coil of the charging pad and the secondary coil of the load are directly overlapped for maximum mutual coupling, some products based on this approach use magnets and visible marks on the charging pad and a piece of metal (magnetic attractor) inside the load for magnetic attraction in order to keep the load in the right location on the charging pad [see Fig. 1(a)]. The advantage of this "guided-positioning" approach is its simplicity. However, the use of the magnet and, hence, the fixed-positioning requirement makes this approach relatively less user friendly. The requirement of a piece of metallic magnetic attractor in the device implies some extra space requirement and induced eddy-current-related power loss (and thus temperature rise) in the magnetic attractor.

Approach 2 is a one-to-one charging method that relies on a mechanically movable primary coil underneath the charging surface as shown in Fig. 1(b). This approach involves a search for the load position (i.e., the secondary coil in the load), either by inductive or capacitive means. The two motors underneath the charging surface will move the primary coil underneath the secondary coil of the load. From the consumers' point of view, this method is a "free-positioning" one because a device can be placed anywhere on the charging surface and the primary coil will be moved below the detected device by the electric motors. In an electric sense, this is equivalent to the "one-to-one" and "fixed-positioning" approach as described for Approach 1. This approach is simple if the charging pad is designed for only one device (i.e., single-device charging). For multiple-load charging, the motor control for the primary coils could be very complex and costly. In addition, systems with movable mechanical parts tend to be less reliable.

Approach 3 adopted in the Qi standard allows the users to place one or more portable electronic devices on the charging surface regardless of their positions and orientations. Instead of the parallel-flux approach [19], [20], the "vertical-flux" approach [20]–[24] is endorsed in the Qi version 1.0 standard. The vertical-flux method can utilize the entire charging surface for energy transfer and has no restriction on the orientation of the receiver coil. Originated from the coreless planar transformer technology [2]–[7], [17], [20] in which energy is transferred from the planar primary winding printed on one side of the printed circuit board (PCB) "vertically" to the secondary winding printed on the other side of the PCB, the vertical-flux idea has been successfully demonstrated in an isolated gate-drive circuit [4], [5] and later implemented in integrated circuits [11], [12] and planar power converters [6], wirelessly powering a lighting device by Philips Research [10] and charging a mobile phone in a "fixed-positioning" manner [7]. By extending the planar winding into a multilayer winding array structure [8], [23] and selectively activating the appropriate coils for localized charging [9], [24], Approach 3 [see Fig. 1(c)] offers "multiple" and "free-positioning" wireless charging. Compared with Approaches 1 and 2, Approach 3 offers more user-friendliness at the expense of relatively more complex winding structure and control electronics.

From the viewpoint of user convenience and safety, free-positioning and localized charging are attractive and user-friendly features. In this paper, a single-layer winding array with ferrite cores [24] is proposed for a free-positioning charging platform with a localized charging feature. This paper is an extended and improved version of [30]. Free positioning utilizes the mathematical packing theory to ensure that the receiver (secondary coil) can be placed freely above the charging platform and yet with sufficiently high energy efficiency. Localized charging means that only the charging area underneath the load (i.e., area enclosed by the receiver coil) on the charging platform is energized. This important feature is essential to the safety requirement of the Qi standard because any noncompliant object, such as a cigarette lighter, when placed on the charging surface must not be affected. The important parameters of the winding array are studied with finite-element analysis (FEA) software and circuit analysis in order to obtain an optimal design for power transfer. Practical measurements are included for evaluation.

II. Winding Array Structure Based on Mathematical Packing Theory

A. Winding Dimensional Relationship Based on Packing Theory

The novelty in this proposal is that the dimensional relationship of the transmitter coil and the receiver coil must be that the receiver coil must be able to fully enclose at least one primary coil [24] regardless of where the receiver coil is placed. The three necessary conditions proposed for the winding areas are as follows: 1) The receiver winding should be larger than the transmitter windings; 2) the receiver winding must fully cover at least one transmitter winding wherever the electronic load is placed on the charging surface of the charging pad; and 3) one transmitter winding is sufficient to provide enough power transfer for the electronic loads under consideration for the charging pad. In this illustration, we assume that the receiver winding is circular. However, it must be pointed out that the receiver winding can be of any polygonal shape such as oval, rectangular, or hexagonal shape.

Fig. 2 shows the typical examples of receiver windings of rectangular and circular shapes. The receiver winding is embedded inside the electronic load for mutual coupling with the transmitter winding. In other words, the transmitter winding is equivalent to the primary winding of a transformer, and the receiver winding is equivalent to the secondary winding.

Let us first consider using circular spiral windings arranged in square packing [26], as shown in Fig. 3. The diameter of the transmitter winding is denoted as d, and that of the receiver winding is denoted as D. The arrangement shown in Fig. 3 is such that a slight movement of the large receiver winding in

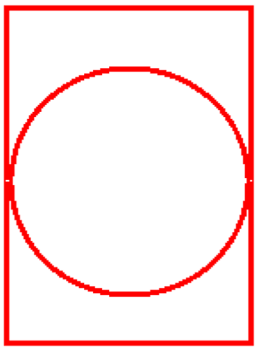

Fig. 2. Two examples of receiver windings (typically of rectangular or circular shape).

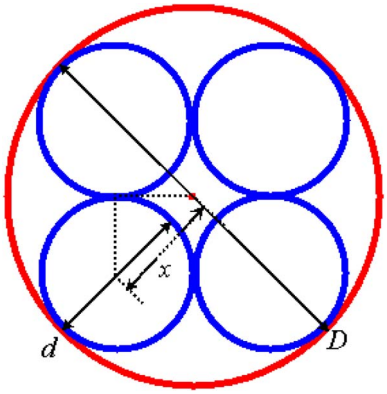

Fig. 3. Dimensional relationship between the (large) receiver and (small) transmitter windings, based on the square packing of circular spiral windings. (The large circle represents the circular receiver winding, and the small circles represent circular transmitter spiral windings.)

any direction will always enclose or cover at least one small transmitter winding. As shown in Fig. 3, x has the relationship with d, as given by

$$x = \sqrt{2} \cdot \frac{d}{2}. \tag{1}$$

Then, the diameter of the receiver winding D can be expressed by

$$D = \frac{d}{2} + x + x + \frac{d}{2} = (1 + \sqrt{2})d. \tag{2}$$

The area ratio between one receiver winding and a transmitter winding is

$$\frac{A_{\text{receiver}}}{A_{\text{transmitter}}} = \frac{\pi(D/2)^2}{\pi(d/2)^2} = \frac{D^2}{d^2} = (1 + \sqrt{2})^2 \approx 5.8284. \tag{3}$$

Using the same argument, other transmitter windings with other shapes and packing methods can be considered. For example, Fig. 4 shows a hexagonal packing of hexagonal spiral transmitter windings. Again, any slight movement of the large circular receiver winding in any direction will ensure that at least one transmitter winding is enclosed by the receiver winding. The relationship between D and d is

$$D = 2d. \tag{4}$$

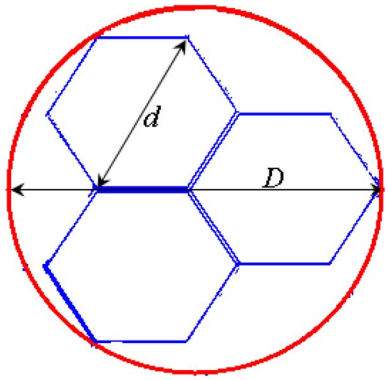

Fig. 4. Dimensional relationship between the (large) receiver and (small) transmitter windings, based on the hexagonal packing of hexagonal spiral windings. (The large circle represents the receiver circular winding, and the small hexagons represent the transmitter hexagonal spiral windings.)

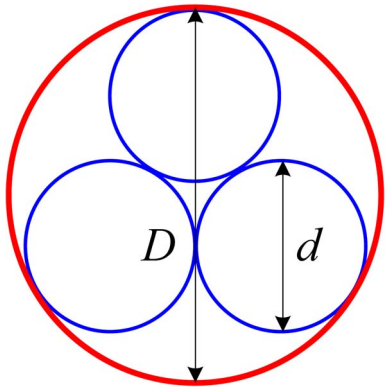

Fig. 5. Dimensional relationship between the (large) receiver and (small) transmitter windings, based on the hexagonal packing of solenoids. (The large circle represents the receiver winding, and the small circles represent the transmitter solenoids.)

The area ratio between one receiver winding and a transmitter winding is

$$\frac{A_{\text{receiver}}}{A_{\text{transmitter}}} = \frac{\pi\dfrac{D^2}{4}}{3 \cdot \dfrac{d}{2} \cdot \dfrac{d}{2} \cdot \dfrac{\sqrt{3}}{2}} = \frac{2\pi}{3\sqrt{3}} \left(\frac{D}{d}\right)^2 \approx 4.8368. \tag{5}$$

Fig. 5 shows a hexagonal packing of circular transmitter solenoids, which is the winding structure studied in this paper. Again, the relationship between D and d is

$$D = \left(1 + \frac{2}{\sqrt{3}}\right) d. \tag{6}$$

The area ratio between one receiver winding and a transmitter winding is

$$\frac{A_{\text{receiver}}}{A_{\text{transmitter}}} = \frac{D^2}{d^2} = (1 + 2/\sqrt{3})^2 \approx 4.6427. \tag{7}$$

Equation (7) shows that the winding structure in Fig. 5 is the best in the three structures shown in Figs. 3–5 because its area ratio is the lowest.

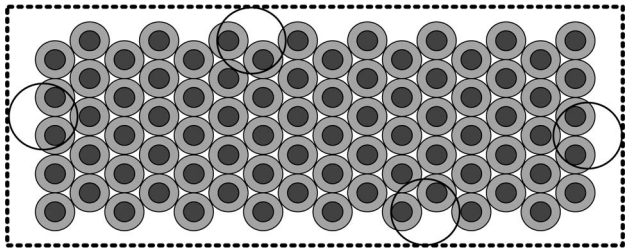

Fig. 6. Single layer of hexagonally packed primary winding array.

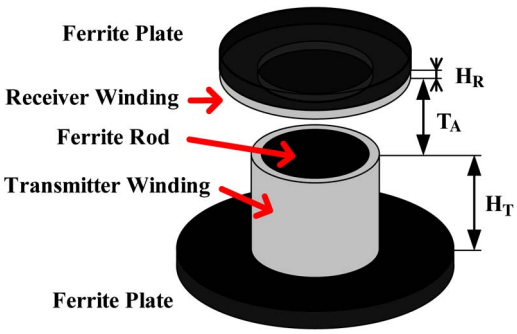

Fig. 7. Three-dimensional model with one transmitter winding.

B. Practical Design Example of Single-Layer Primary Winding Array Structure

Fig. 6 shows the transmitter (primary) winding array structure of the proposed charging platform. Fig. 7 shows a 3-D model of one charging unit. The charging platform shown in Fig. 7 contains a transmitter ferrite plate (bottom), a transmitter core, a transmitter winding, a receiver winding, and a receiver ferrite plate (top), where H_T is the height of the transmitter core and winding, H_R is the height of the receiver winding, and T_A is the thickness of the airgap between two windings. Fig. 8 shows the dimensional relationship between the transmitter and receiver windings. It is guaranteed that the inner edge of the receiver winding is able to cover three transmitter cores. Therefore, the relationship of the parameters shown in Fig. 8 can be given by

$$R_R = \frac{(2+\sqrt{3})R_{TC} + 2T_T + D}{\sqrt{3}} \tag{8}$$

where R_{TC} is the radius of the transmitter core; T_T is the thickness of the transmitter winding; R_R is the inner radius of the receiver winding; T_R is the thickness of the receiver winding; and D is the distance between two transmitter windings.

III. FEA and Circuit Model

A. FEA Models

The mutual inductance between two parallel planar coils will change with their relative position [29]. Likewise, the mutual coupling of the receiver coil and the transmitter coil in the proposed charging platform will change with their relative position. In general, the mutual inductance is highest when the transmitter and receiver coils share the same center. Figs. 9 and 10 show the best and worst coupling position schematics, respectively. Magnetostatic analyses are applied to a small model and a large model, respectively, and the simulation results are compared to check if a small model is accurate enough to represent the whole platform. Figs. 11(a) and 12(a) show the small models of the best and worst positions, respectively. Figs. 11(b) and 12(b) show the large models for the best coupling position and the worst coupling position, respectively.

The parameters used in the simulations are based on the practical sizes of the ferrite rods wounded with litz wire. The parameters of the charging platform are listed in Table I. The simulation results are included in Table II, where L_T and R_T are the inductance and ac resistance of the transmitter winding, respectively; L_R and R_R are the inductance and

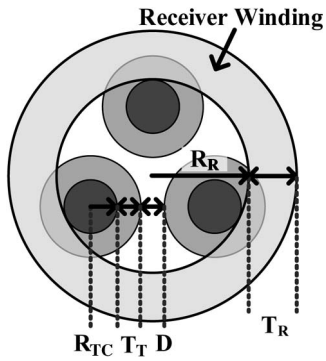

Fig. 8. Top view and parameters of the charging platform.

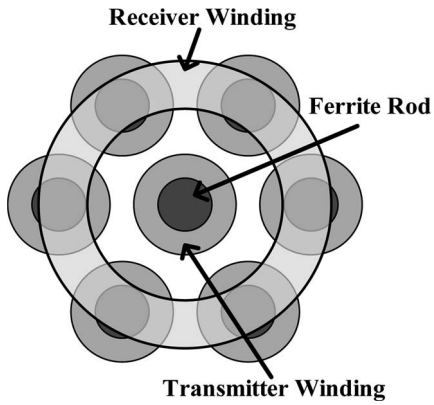

Fig. 9. Best coupling position for mutual coupling.

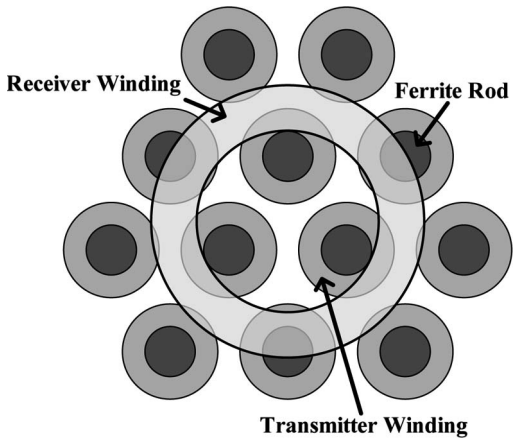

Fig. 10. Worst coupling position for mutual coupling.

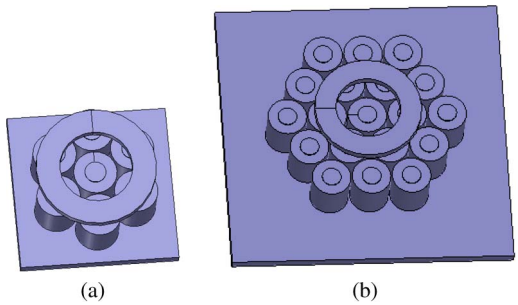

Fig. 11. (a) Small and (b) large models at the best position.

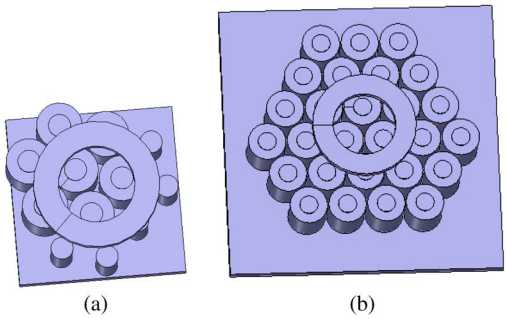

Fig. 12. (a) Small and (b) large models at the worst position.

TABLE I
PARAMETERS OF THE CHARGING PLATFORM

Transmitter winding structure	12 turns × 4 layers	Ferrite matieral	F material (Magnetics Inc.)
Receiver winding structure	2turns × 8 layers	Ferrite core size	H_T 9 mm; R_{TC} 2mm
Litz wire structure	10 strands × 36 AWG	Top & bottom ferrite plates size	30mm×30mm×2mm
H_R	1.5 mm	T_T	0.56 mm × 4 layers
T_A	1.5 mm	T_R	0.56 mm × 8 layers
R_R	6.91 mm	D	0 mm

ac resistance of the receiver winding, respectively; k is the coupling coefficient of the two windings; R_m is the mutual resistance of the two windings defined in [27] to account for the eddy-current losses in the windings caused by the coupled ac magnetic field.

Here, litz wire is used in the coils, and thus, the method reported in [28] can be used for calculating the ac resistance with the aid of finite-element magnetostatic analysis. The main concept in this method is that the ac resistance is only decided by the B-field and the operating frequency as long as the wire is a litz wire or the wire cross-sectional diameter is small enough when compared with the skin depth so that the current density of the winding region can be considered as constant. The simulation results in Table II show that the differences between the parameters of the small and large models are relatively small. Therefore, a small model is good enough to present the characteristics of the whole platform.

TABLE II
SMALL- AND LARGE-MODEL SIMULATION RESULT COMPARISON (AT 150 kHz)

		L_T (μH)	L_R (μH)	k	R_T (Ω)	R_R (Ω)	R_m (Ω)
Best Position	Small Model	70.65	14.16	0.289	0.859	0.201	0.039
	Large Model	71.38	15.62	0.308	0.862	0.212	0.043
Worst Position	Small Model	71.05	14.92	0.253	0.886	0.198	0.035
	Large Model	71.49	15.77	0.264	0.891	0.209	0.023

TABLE III
CORE LOSS SIMULATION RESULTS

	F(kHz)	Input Current (A) RMS	Output Current (A) RMS	Output Power/W (R_{LOAD} 5Ω)	Core Loss (W)
Best Position	150	0.91	1.53	11.8	0.116
Worst Position	150	0.66	0.99	4.9	0.051

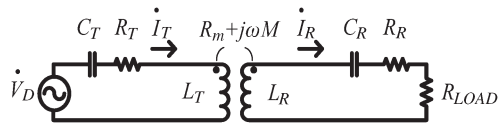

Fig. 13. Simplified equivalent circuit for the charging system with core loss neglected.

B. Core Loss Estimation Based on FEA

Using the data of the F material in the Maxwell FEA software as an example, transient analysis has been carried out to determine the core loss of the charging system for both the best position and the worst position based on the small models. The results are listed in Table III. It is obvious that the core loss is small enough compared with the load, and it can be neglected to allow a simpler circuit model of the proposed charging system.

C. Equivalent Circuit Analysis With Core Loss Neglected

The whole charging system can be represented by the equivalent circuit in Fig. 13 [27]. Here, M is the mutual inductance of the two windings, and C_T and C_R are the resonant capacitors for the transmitter and the receiver, respectively. The efficiency η of the system can be determined through the following equations:

$$(j\omega M + R_m)\dot{I}_T = \left(j\omega L_R - j\frac{1}{\omega C_R} + R_R + R_{\text{LOAD}}\right)\dot{I}_R \tag{9}$$

$$a = \frac{\dot{I}_T}{\dot{I}_R} = \frac{j\left(\omega L_R - \frac{1}{\omega C_R}\right) + R_R + R_{\text{LOAD}}}{j\omega M + R_m} \tag{10}$$

where $\dot{I}_T$ and $\dot{I}_R$ are the complex currents of the transmitter and receiver equivalent circuit in Fig. 13, and

$$\begin{aligned}\eta &= \frac{P_{\mathrm{LOAD}}}{P_{\mathrm{TOTAL}}} \\ &= \frac{I_R^2 R_{\mathrm{LOAD}}}{I_T^2 R_T + I_R^2 (R_R + R_{\mathrm{LOAD}}) - 2(\dot{I}_T \cdot \dot{I}_R) R_m} \\ &= \frac{R_{\mathrm{LOAD}}}{|a|^2 R_T + R_T + R_{\mathrm{LOAD}} - 2\mathrm{Re}(a) \cdot R_m} \end{aligned} \tag{11}$$

where $\mathrm{Re}(a)$ is the real part of a.

Apply Kirchhoff's voltage law in the primary side

$$\dot{V}_D = \dot{I}_T \left(j \left(\omega L_T - \frac{1}{\omega C_T} \right) + R_T \right) - \dot{I}_R (j\omega M + R_m). \tag{12}$$

The voltage gain G_v and current gain G_i can be expressed by

$$\begin{aligned} G_v &= \frac{|v_{\mathrm{LOAD}}|}{|v_d|} \\ &= \frac{R_{\mathrm{LOAD}}}{\left| a \cdot \left(j \left(\omega L_T - \frac{1}{\omega C_T} \right) + R_T \right) - (j\omega M + R_m) \right|} \end{aligned} \tag{13}$$

$$G_i = \frac{|\dot{I}_R|}{|\dot{I}_T|} = \frac{1}{|a|}. \tag{14}$$

If the receiver resonant capacitor is not added, (10) can be expressed as

$$|a| = \frac{\sqrt{(R_R + R_{\mathrm{LOAD}})^2 + \omega^2 L_R^2}}{\sqrt{\omega^2 M^2 + R_m^2}} \tag{15}$$

$$\mathrm{Re}(a) = \frac{(R_R + R_{\mathrm{LOAD}}) R_m + \omega^2 L_R M}{\omega^2 M^2 + R_m^2}. \tag{16}$$

If the system is operating at the receiver's resonant frequency, then

$$|a| = \frac{R_R + R_{\mathrm{LOAD}}}{\sqrt{\omega^2 M^2 + R_m^2}} \tag{17}$$

$$\mathrm{Re}(a) = \frac{(R_R + R_{\mathrm{LOAD}}) R_m}{\omega^2 M^2 + R_m^2}. \tag{18}$$

The difference between the denominators of (11) when without receiver resonance and with receiver resonance can be worked out as

$$\Delta = \frac{\omega^2 L_R (L_R R_T - M R_m)}{\omega^2 M^2 + R_m^2}. \tag{19}$$

This term is positive because L_R is larger than M and R_T is larger than R_m according to the analysis in Section III-B. Therefore, with a chosen operating frequency, the receiver resonance can raise the power transfer efficiency of the system. By doing a similar comparison, the following conclusions can be made.

1) Receiver resonance can increase the current gain.

Fig. 14. (Left) Worst position and (right) best position core arrays.

Fig. 15. (Left) Worst position and (right) best position winding arrays.

Fig. 16. Receiver winding and receiver ferrite plate.

2) Both transmitter resonance and receiver resonance can increase the voltage gain.

IV. Experiment Verification

Because the ferrite material used in the FEA was not available during the tests, some small ferrite rods used for making small inductors were used to construct the single-layer winding array structure. It is therefore important to note that the measurements and simulations may not agree exactly because the ferrite materials used in the simulation and the practical prototype are not the same. Nevertheless, their results should not affect the evaluation of the proposed single-layer winding array structure and its potential as a new version of wireless charging system.

Figs. 14–16 show the experimental prototypes for both the best position and worst position models. It should be noted that the ferrite material used in the prototype is not the F material used in the simulation. However, the airgap T_A is 1.5 mm in the prototype. The reluctance in the airgap is therefore the dominant reluctance in the magnetic path because the reluctance in the magnetic core is relatively small. As long as the magnetic

TABLE IV
INDUCTANCE AND COUPLING COEFFICIENT COMPARISON BETWEEN SIMULATION AND MEASURED RESULTS

		L_T (μH)	L_R (μH)	k
Best Position	Simulation	70.65	14.16	0.289
	Measured (150kHz)	68.01	14.41	0.285
Worst Position	Simulation	71.05	14.92	0.253
	Measured (150kHz)	70.22	14.93	0.242

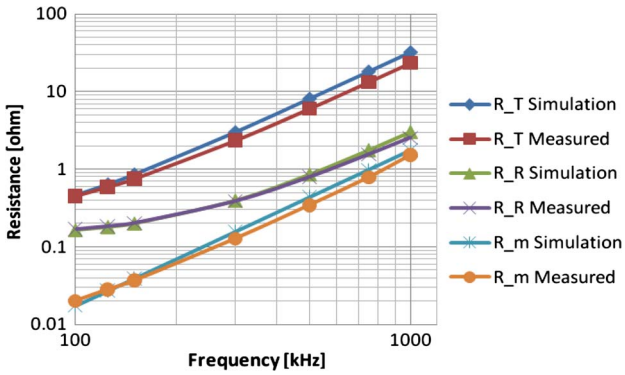

Fig. 17. Resistance comparison between the simulation and measured results of the best position.

cores are not saturated, the practical results are expected to be close to that of the simulations because of the airgap between the transmitter and the receiver. This point can be confirmed from the comparison of results in Table IV.

The simulation and measured results are shown in Table IV and Figs. 17 and 18 in which all the parameters in the circuit model derived in Section III are included. It is clear that the differences between the calculated and measured winding parameters (i.e., inductances and coupling coefficients) are very small, implying that the efficiency of the practical charging platform should be very close to that of the simulation results (provided that the practical and simulated core losses are close to each other). Fig. 19 shows the simulated and measured results of the energy efficiency. It can be observed that the frequency range of 125–150 kHz is the optimal operating frequency with efficiencies of over 85% in the best and worst positions. This is the typical operating frequency acceptable in the version 1.0 of the Qi wireless power transfer standard. The slight difference in the measured and simulated energy efficiencies is expected because the F-core material used in the simulation and the actual ferrite rods used in practice are not identical, and therefore, their core losses are not identical. The reduction in energy efficiency, with increasing operating frequency in the practical measurements, is likely due to the increasing core losses that are not accounted for precisely in the simulation by the F-core material. However, the chosen frequency range is 125–150 kHz in this case, and the energy efficiency remains high in this frequency range. The small variation of energy efficiency between the best and worst positions is practically confirmed.

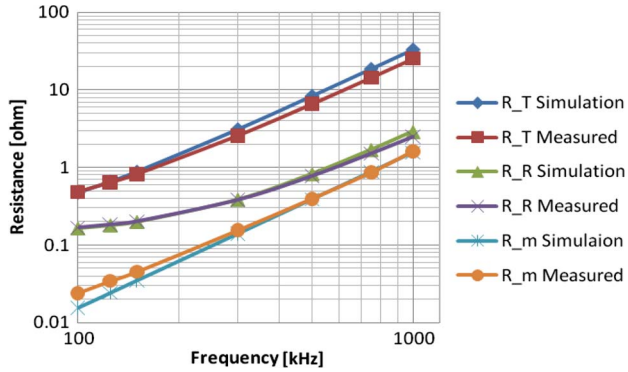

Fig. 18. Resistance comparison between the simulation and measured results of the best position.

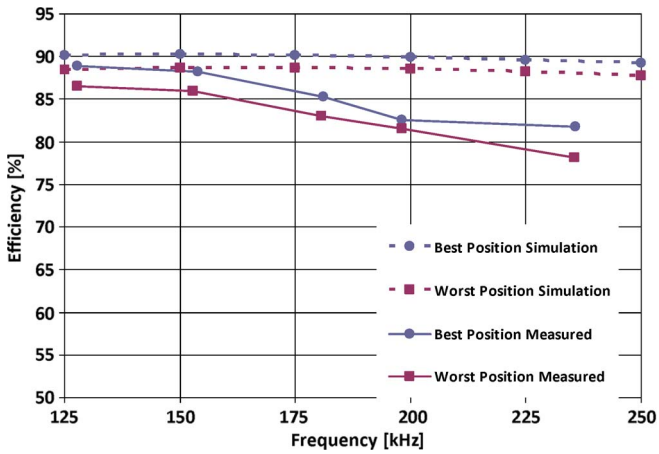

Fig. 19. Simulated and measured efficiencies as a function of operation frequency.

V. DISCUSSION

The packing theory presented in Section II provides a guideline to the design of the wireless charging system. In practice, the size of the receiver coil is restricted by the surface area of the electronic device to be charged. Thus, the first factor to be determined is the dimension of the receiver coil. For devices like mobile phones, the Qi standard document specifies such dimensions for the receiver coil. Once the dimension of the receiver coil is known, the diameters of the magnetic cores and the space required for the practical transmitter windings can be determined by the packing theory.

VI. CONCLUSION

An investigation into a single-layer winding array structure with a patented geometric relationship between the transmitter and receiver coils is presented. This winding array structure is particularly suitable for wireless charging with the user-friendly free-positioning and localized charging features. The mathematical packing theory is used to explain the hexagonal packing structure as the optimal geometric winding array structure for this application. The novel winding arrangement is that the receiver coil always encloses fully at least one transmitter coil regardless of where it is placed within the charging area. Detailed circuit analysis covering the best and

worst magnetically coupled positions is included and supported with FEA. Practical measurements have confirmed that energy efficiency in the range of 86%–89% is possible for any position between the worst and best magnetically coupled positions even when low-cost ferrite rods are used for constructing the single-layer winding array magnetic structure. The small variation (3%) of energy efficiency between the best and worst positions means that the proposed single-layer winding array structure offers free-positioning charging without significantly sacrifying the energy efficiency. The proposal offers a new version of wireless charging system for the Qi wireless power transfer standard. So far, the version 1.0 of the Qi standard is set for wireless power charging of up to 5 W. However, active wireless power transfer projects [31], [32] have recently been reported for medium-power applications. It is envisaged that the international engineering communities should work together to set up an international standard for high-power applications in wireless power transfer.

ACKNOWLEDGMENT

The authors would like to thank ConvenientPower HK, Ltd. for its permission to use some materials from [24].

REFERENCES

[1] [Online]. Available: http://www.wirelesspowerconsortium.com
[2] S. C. Tang, S. Y. R. Hui, and H. Chung, "Coreless printed circuit board (PCB) transformers with high power density and high efficiency," *Electron. Lett.*, vol. 36, no. 11, pp. 943–944, May 2000.
[3] S. C. Tang, S. Y. R. Hui, and H. Chung, "Coreless planar printed-circuit-board (PCB) transformers—A fundamental concept for signal and energy transfer," *IEEE Trans. Power Electron.*, vol. 15, no. 5, pp. 931–941, Sep. 2000.
[4] S. Y. Hui, H. S. Chung, and S. C. Tang, "Coreless printed circuit board (PCB) transformers for power MOSFET/IGBT gate drive circuits," *IEEE Trans. Power Electron.*, vol. 14, no. 3, pp. 422–430, May 1999.
[5] S. C. Tang, S. Y. R. Hui, and H. Chung, "Optimal operation of coreless PCB transformer-isolated gate drive circuits with wide switching frequency range," *IEEE Trans. Power Electron.*, vol. 14, no. 3, pp. 506–514, May 1999.
[6] S. C. Tang, S. Y. R. Hui, and H. Chung, "A low-profile low-power converter using coreless PCB transformer with ferrite polymer composite," *IEEE Trans. Power Electron.*, vol. 16, no. 4, pp. 493–498, Jul. 2001.
[7] B. Choi, J. Nho, H. Cha, T. Ahn, and S. Choi, "Design and implementation of low-profile contactless battery charger using planar printed circuit board windings as energy transfer device," *IEEE Trans. Ind. Electron.*, vol. 51, no. 1, pp. 140–147, Feb. 2004.
[8] S. Y. R. Hui and W. C. Ho, "A new generation of universal contactless battery charging platform for portable consumer electronic equipment," *IEEE Trans. Power Electron.*, vol. 20, no. 3, pp. 620–627, May 2005.
[9] X. Liu and S. Y. R. Hui, "Simulation study and experimental verification of a contactless battery charging platform with localized charging features," *IEEE Trans. Power Electron.*, vol. 22, no. 6, pp. 2202–2210, Nov. 2007.
[10] E. Waffenschmidt and B. Ackermann, "Size advantage of coreless transformers in the MHz range," presented at the EPE, 2001, paper DS2-9.
[11] M. Munzer, W. Ademmer, B. Strzalkowski, and K. T. Kaschani, "Insulated signal transfer in a half bridge driver IC based on coreless transformer technology," in *Proc. 5th Int. Conf. Power Electron. Drive Syst. PEDS*, 2003, vol. 1, pp. 93–96.
[12] P. Luniewski and U. Jansen, "Unsymmetrical gate voltage drive for high power 1200V IGBT4 modules based on coreless transformer technology driver," in *Proc. 13th Power Electron. Motion Control Conf., EPE-PEM*, 2008, pp. 88–96.
[13] X. Liu, W. M. Ng, C. K. Lee, and S. Y. R. Hui, "Optimal operation of contactless transformers with resonance at secondary circuit," in *Proc. 23th IEEE Annu. Appl. Power Electron. Spec. Conf.*, Feb. 2008, pp. 645–650.
[14] E. Waffenschmidt and T. Staring, "Limitation of inductive power transfer for consumer applications," in *Proc. 13th Eur. Conf. Power Electron. Appl.*, 2009, pp. 1–10.
[15] P. Hothongkham and V. Kinnares, "High-voltage high-frequency power supply using phase shift PWM full bridge inverter fed ozone generator," in *Proc. IEEE Int. Symp. Ind. Electron.*, Jul. 5–8, 2009, pp. 1817–1822.
[16] Z. M. Ye, P. K. Jain, and P. C. Sen, "A full bridge resonant inverter with modified phase shift modulation," in *Proc. IEEE 36th Power Electron. Spec. Conf.*, Jun. 16, 2005, pp. 642–649.
[17] S. Y. R. Hui and S. C. Tang, "Coreless printed-circuit-board (PCB) transformers and operating techniques therefor," EU Patent EP(GB)0 935 263B, May 26, 2004.
[18] L. Cheng, J. Hay, and P. Beart, "Contactless power transfer," U.S. Patent 6 906 495, Jun. 14, 2005.
[19] L. Cheng, J. Hay, and P. Beart, "Primary units, methods and systems for contactless power transfer," U.S. Patent 7 239 110, Jul. 3, 2007.
[20] S. Y. R. Hui and S. C. Tang, "Planar printed circuit-board transformers with effective electromagnetic interference (EMI) shielding," U.S. Patent 6 501 364, Dec. 31, 2002.
[21] S. Y. R. Hui, "Planar inductive battery charger," British Patent GB2 389 720, Sep. 7, 2005.
[22] S. Y. R. Hui, "Apparatus for energy transfer by induction," British Patent GB2 389 767, Apr. 19, 2006.
[23] S. Y. R. Hui, "Inductive battery charger system with primary transformer windings formed in a multi-layer structure," U.S. Patent 7 164 255, Jan. 16, 2007.
[24] S. Y. R. Hui, W. C. Ho, X. Liu, and W. C. Chan, "Localized charging, load identification and bi-directional communication methods for a planar inductive battery charging pad," U.S. Patent 7915858, Mar. 29, 2011.
[25] S. Y. R. Hui and W. C. Ho, "Power transfer device and method," U.S. Patent Application 12/705 911, Feb. 15, 2010.
[26] Wolfram Math World, Circle Packing. [Online]. Available: http://mathworld.com/circlepacking.html
[27] H. Spreen, "Electrical terminal representation of conductor loss in transformers," *IEEE Trans. Power Electron.*, vol. 5, no. 4, pp. 424–429, Oct. 1990.
[28] C. R. Sullivan, "Computationally efficient winding loss calculation with multiple windings, arbitrary waveforms, and two-dimensional or three-dimensional field geometry," *IEEE Trans. Power Electron.*, vol. 16, no. 1, pp. 142–150, Jan. 2001.
[29] Y. P. Su, X. Liu, and S. Y. R. Hui, "Mutual inductance calculation of movable planar coils on parallel surfaces," *IEEE Trans. Power Electron.*, vol. 24, no. 4, pp. 1115–1123, Apr. 2009.
[30] W. X. Zhong, X. Liu, and S. Y. R. Hui, "Analysis on a single-layer winding array structure for contactless battery charging systems with free-positioning and localized charging features," in *Proc. IEEE Energy Convers. Congr. Expo. (ECCE)*, 2010, pp. 658–665.
[31] A. J. Moradewicz and M. P. Kazmierkowski, "Contactless energy transfer system with FPGA-controlled resonant converter," *IEEE Trans. Ind. Electron.*, vol. 57, no. 9, pp. 3181–3190, Sep. 2010.
[32] G. Elliott, S. Raabe, G. A. Covic, and J. T. Boys, "Multiphase pickups for large lateral tolerance contactless power-transfer systems," *IEEE Trans. Ind. Electron.*, vol. 57, no. 5, pp. 1590–1598, May 2010.

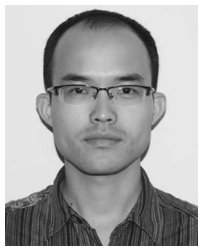

W. X. Zhong was born in China in 1984. He received the B.S. degree in electrical engineering from Tsinghua University, Beijing, China, in 2007. He is currently working toward the Ph.D. degree in the Center for Power Electronics, City University of Hong Kong, Kowloon, Hong Kong.

His current research interests include synchronous rectification and wireless power transfer.

Xun Liu (M'07) was born in China in 1978. He received the B.S. and M.S. degrees in electrical engineering from Tsinghua University, Beijing, China, in 2001 and 2003, respectively, and the Ph.D. degree from the City University of Hong Kong, Beijing, in 2007.

He is currently the Chief Technology Officer with ConvenientPower HK Ltd., Shatin, Hong Kong, where he is leading the research, innovation, and standardization of a new generation of universal wireless charging platform for a wide range of consumer electronic products. His current research interest is power electromagnetics.

Dr. Liu is the Vice-Chair of the Specification Work Group in the Wireless Power Consortium. He was the recipient of the 2009 IEEE Power Electronics Society Transaction Prize Paper Award.

S. Y. Ron Hui (F'03) received the B.Sc.Eng. degree (Hons) from the University of Birmingham, Birmingham, U.K., in 1984, and the D.I.C. and Ph.D. degrees from the Imperial College of Science and Technology, London, U.K., in 1987.

He was a Lecturer with the University of Nottingham, Nottingham, U.K., in 1987–1990. In 1990, he was with the University of Technology, Sydney, Australia, and was appointed Senior Lecturer with the University of Sydney, Sydney, in 1992, where he became a Reader in 1995. He joined the City University of Hong Kong (CityU), Kowloon, Hong Kong, as a Professor in 1996 and was promoted to Chair Professor in 1998. In 2001–2004, he served as an Associate Dean of the Faculty of Science and Engineering, CityU. From 2010, he holds the Chair Professorship with both CityU and Imperial College London, London. He has published over 200 technical papers, including more than 140 refereed journal publications and book chapters. Over 45 of his patents have been adopted by industry.

Dr. Hui is a Fellow of The Institution of Engineering and Technology (IET). He has been an Associate Editor (Power Conversion) of the IEEE TRANSACTIONS ON POWER ELECTRONICS since 1997 and an Associate Editor (Lighting Technology) of the IEEE TRANSACTIONS ON INDUSTRIAL ELECTRONICS since 2007. He was recognized twice as an IEEE Distinguished Lecturer by the IEEE Power Electronics Society in 2004 and 2006. He served as one of the 18 Administrative Committee members of the IEEE Power Electronics Society and was the Chairman of its Constitution and Bylaws Committee from 2002–2010. He was the recipient of the Teaching Excellence Award at CityU in 1998 and the Earth Champion Award in 2008. He was the recipient of the IEEE Best Paper Award from the IEEE Industry Applications Society Committee on Production and Applications of Light in 2002 and two IEEE POWER ELECTRONICS TRANSACTIONS Prize Paper Awards for his publication in wireless battery charging platform technology in 2009 and for his paper on the light-emitting-diode system theory in 2010. His inventions on wireless charging platform technology underpin the dimensions of the international wireless charging standard "Qi" for the wireless charging of consumer electronics with free-positioning, localized charging and load identification features. In November 2010, he was the recipient of the IEEE Rudolf Chope R&D Award from the IEEE Industrial Electronics Society and the IET Achievement Medal (The Crompton Medal) and was elected to the Fellowship of the Australian Academy of Technological Sciences & Engineering.